Vertical Normal Mode Transforms: Theory and Application

SCOTT R. FULTON AND WAYNE H. SCHUBERT

Department of Atmospheric Science, Colorado State University, Fort Collins, CO 80523

(Manuscript received 18 June 1984, in final form 5 September 1984)

ABSTRACT

The separation of the vertical structure of the solutions of the primitive (hydrostatic) meteorological equations is formalized as a vertical normal-mode transform. The transform is implemented for arbitrary static stability profiles by the Rayleigh–Ritz method, which is based on a variational formulation closely connected with energetics. With polynomial basis functions the order of accuracy is exponential. When vertical transforms of observed fields are computed, energy may be aliased onto the wrong vertical modes; this aliasing may be reduced substantially by a careful choice of sampling levels. The spectral distributions of observed tropical forcings of the wind and mass fields are presented.

1. Introduction

The action of gravity makes the vertical dimension of the atmosphere fundamentally different than the horizontal. In many problems it is convenient to separate the vertical structure of the motion from the horizontal structure. Lamb (1932, Articles 311–312) used this idea in studying long waves in the atmosphere and gave references to earlier work of a similar nature. Taylor (1936) was perhaps the first to show that a compressible atmosphere may support free oscillations with several different vertical structures; each of these modes has the horizontal structure of the motions of an incompressible fluid with depth equal to a different value of the separation constant, for which he introduced the term "equivalent depth." Since that time this concept has been applied in the study of atmospheric tides (Siebert, 1961; Chapman and Lindzen, 1970), atmospheric waves (Jacobs and Wiin-Nielsen, 1966; Lindzen, 1967; Wiin-Nielsen, 1971a,b), geostrophic adjustment (Fulton and Schubert, 1980; Silva Dias *et al.*, 1983), normal mode initialization (Daley, 1981; Kasahara and Shigehisa, 1983), and the formulation of lateral boundary conditions (Oliger and Sundström, 1978; Hack and Schubert, 1981)—to name only a few of the many applications.

In the standard separation of variables each of the dependent variables is represented as a horizontally varying part times a vertically varying part. Substitution into the governing equations then yields separate equations for the horizontal and vertical structures, which are related by the separation constant. The solutions of the vertical structure equation with appropriate boundary conditions are shown to form a complete set, and thus the dependent variables can be expanded in terms of them. An alternate approach formalizes the separation of vertical structure as a vertical normal mode transform (Silva Dias *et al.*, 1983), yielding the same vertical structure problem and normal mode expansions without assuming separation of variables. In this way the connection between the primitive (hydrostatic) meteorological equations and the shallow water equations is made explicit. This vertical transform and its implementation in practice are the subject of this paper.

When using realistic stability profiles the vertical structure problem must be discretized and solved numerically. Often this has been accomplished by discretizing the governing equations and computing the normal modes of the discretized system (e.g., Temperton, 1984), leading to discrete forms of the transform. In this paper we derive the transform in its vertically continuous form instead, and then discretize that directly. In Section 2 we review the formulation of the transform and discuss its properties, independent of discretization. The approximate solution of the vertical structure problem and the implementation of the transform are discussed in Section 3. In Section 4 we consider the questions of accuracy and aliasing, and then apply the transform to observed sources of heat and vorticity using observed stability profiles. Concluding remarks are given in Section 5.

2. Theory

In this section we review the vertical transform and its properties. The discussion is independent of geometrical or dynamical approximations in the horizontal (e.g., f-plane, β-plane, quasi-geostrophy, etc.). We use pressure as the vertical coordinate, since the

corresponding weight function (pseudodensity) in the natural vertical inner product is constant, but the problem may be formulated similarly in terms of log pressure (Silva Dias *et al.*, 1983), sigma coordinates (Kasahara and Puri, 1981) or physical height (Oliger and Sundström, 1978).

a. Governing equations and boundary conditions

Consider the motions of a compressible atmosphere in hydrostatic balance. The horizontal momentum, hydrostatic, continuity and thermodynamic energy equations may be written as

$$\frac{\partial \mathbf{v}}{\partial t} + f\mathbf{k} \times \mathbf{v} + \nabla\phi = \mathbf{F}, \tag{2.1a}$$

$$\frac{\partial \phi}{\partial p} + \frac{RT}{p} = 0, \tag{2.1b}$$

$$\nabla \cdot \mathbf{v} + \frac{\partial \omega}{\partial p} = 0, \tag{2.1c}$$

$$c_p \frac{\partial T}{\partial t} - \frac{p\sigma}{\kappa}\omega = Q, \tag{2.1d}$$

with the following definitions:

p	pressure
t	time
$\mathbf{v}$	horizontal velocity
ω	vertical p-velocity
T	deviation of temperature from $\bar{T}(p)$
ϕ	deviation of geopotential from $\bar{\phi}(p)$
$\mathbf{k}$	vertical unit vector
f	Coriolis parameter
R	gas constant for dry air
c_p	specific heat at constant pressure
κ	$=R/c_p$
σ	static stability $[=p^{-2}(\kappa R\bar{T} - pdR\bar{T}/dp)]$
∇	del operator at constant p.

We may regard (2.1a) and (2.1d) as being linearized about the motionless hydrostatic basic state $(\bar{T}, \bar{\phi})$, or may retain the nonlinear terms in $\mathbf{F}$ and Q, which also may include friction or specified forcing terms. The atmosphere is taken to be vertically bounded, with the vertical p-velocity required to vanish at the top boundary $p = p_T \geq 0$ and the actual vertical velocity required to vanish at the bottom boundary $p = p_B$. After linearization these boundary conditions are

$$\left.\begin{aligned} \omega &= 0 \quad \text{at} \quad p = p_T \\ \frac{\partial \phi}{\partial t} - \frac{R\bar{T}}{p}\omega &= 0 \quad \text{at} \quad p = p_B \end{aligned}\right\}. \tag{2.2}$$

Eliminating T and ω between (2.1b)–(2.1d) yields

$$L\left\{\frac{\partial \phi}{\partial t}\right\} + \nabla \cdot \mathbf{v} = L\left\{\frac{\partial \Phi}{\partial t}\right\}. \tag{2.3}$$

Here L is the vertical differential operator

$$L\{\cdot\} = -\frac{\partial}{\partial p}\left[\frac{1}{\sigma}\frac{\partial(\cdot)}{\partial p}\right], \tag{2.4}$$

and the "forced geopotential" Φ, defined by

$$-p\frac{\partial}{\partial p}\left(\frac{\partial \Phi}{\partial t}\right) = \kappa Q, \tag{2.5}$$

is the geopotential which would result from Q if the motion were constrained to be nondivergent. Similarly, eliminating ω from the boundary conditions (2.2) using (2.1b) and (2.1d) yields

$$B_T\left[\frac{\partial \phi}{\partial t} - \frac{\partial \Phi}{\partial t}\right] = B_B\left[\frac{\partial \phi}{\partial t} - \frac{\partial \Phi}{\partial t}\right] = 0, \tag{2.6}$$

where B_T and B_B are the boundary functionals

$$\left.\begin{aligned} B_T[\cdot] &= \left[p\frac{\partial(\cdot)}{\partial p}\right]_{p=p_T} \\ B_B[\cdot] &= \left[p\frac{\partial(\cdot)}{\partial p} + \frac{p^2\sigma}{R\bar{T}}(\cdot)\right]_{p=p_B} \end{aligned}\right\}. \tag{2.7}$$

In obtaining (2.6) we have set $\partial\Phi/\partial t = 0$ at $p = p_B$, thus fixing one of the constants of integration implicit in (2.5).

b. The vertical transform

The only vertical derivatives in the governing equations (2.1a) and (2.3) appear in the term $L\{(\partial\phi/\partial t) - (\partial\Phi/\partial t)\}$. Following Sneddon (1972), the properties of L are used to design the vertical transform in such a way that it eliminates this vertical structure. Defining the vertical inner product

$$\langle u, v\rangle = \frac{1}{p_B - p_T}\int_{p_T}^{p_B} u(p)v(p)dp, \tag{2.8}$$

for any functions u and v of pressure p, we seek an integral transform of the form

$$T[u(p)] = \hat{u}_n = \langle u, \Psi_n\rangle, \tag{2.9}$$

where the kernel $\Psi_n(p)$ of the transform is to be chosen so that

$$T\left[L\left(\frac{\partial \phi}{\partial t} - \frac{\partial \Phi}{\partial t}\right)\right] = \lambda_n\left(\frac{\partial \hat{\phi}_n}{\partial t} - \frac{\partial \hat{\Phi}_n}{\partial t}\right), \tag{2.10}$$

with λ_n a constant. Substituting from (2.4), (2.8) and (2.9) in the left side of (2.10) and integrating by parts twice yields

$$T\left[L\left(\frac{\partial\phi}{\partial t}-\frac{\partial\Phi}{\partial t}\right)\right]$$
$$=\frac{1}{p_B-p_T}\int_{p_T}^{p_B}\left(\frac{\partial\phi}{\partial t}-\frac{\partial\Phi}{\partial t}\right)L\{\Psi_n\}dp$$
$$+\frac{1}{p_B-p_T}\left\{\left[\frac{1}{\sigma}\left(\frac{\partial\phi}{\partial t}-\frac{\partial\Phi}{\partial t}\right)\frac{d\Psi_n}{dp}-\Psi_n\frac{\partial}{\partial p}\left(\frac{\partial\phi}{\partial t}-\frac{\partial\Phi}{\partial t}\right)\right]\right\}_{p_T}^{p_B}. \quad (2.11)$$

The boundary conditions (2.6) then imply that the desired property (2.10) will hold provided that we choose $\Psi_n(p)$ and λ_n as solutions of the vertical structure problem

$$\left.\begin{aligned}L\{\Psi_n(p)\}&=\lambda_n\Psi_n(p)\\ B_T[\Psi_n]&=B_B[\Psi_n]=0\end{aligned}\right\}. \quad (2.12)$$

The theory of Sturm-Liouville eigenvalue problems such as (2.12) is well known (e.g., Courant and Hilbert, 1953; Stakgold, 1979); we use this theory freely in what follows to establish various properties of the vertical transform. In this discussion $C^{(k)}[p_T, p_B]$ will denote the space of all real-valued functions u of pressure p with $d^{(j)}u/dp^j$ continuous on the interval $[p_T, p_B]$ for $j = 0, \ldots, k$. For concreteness we assume that $\sigma \in C^{(1)}[p_T, p_B]$ with $\sigma(p) > 0$ for $p_T \leqslant p \leqslant p_B$, although this assumption may be relaxed somewhat. A natural domain for the operator L is then $D = \{u \in C^{(2)}[p_T, p_B]: B_T[u] = B_B[u] = 0\}$; integrating by parts twice shows $\langle Lu, v\rangle = \langle u, Lv\rangle$ for all u and v in D so L is self-adjoint.

To obtain the inverse vertical transform we use the fact that (2.12) has a countably infinite set of solutions $\{\lambda_n, \Psi_n(p)\}_{n=0}^{\infty}$ with the following properties.

(i) The eigenvalues λ_n are real and satisfy $\lambda_0 < \lambda_1 < \cdots$ with $\lambda_n \to \infty$ as $n \to \infty$;

(ii) The eigenfunctions $\Psi_n(p)$ lie in D and are orthonormal in the inner product (2.8), i.e. $\langle \Psi_m, \Psi_n\rangle = \delta_{mn} = \begin{cases}1 & m = n\\ 0 & m \neq n\end{cases}$;

(iii) The eigenfunctions $\Psi_n(p)$ form a complete set.

Property (iii) means that any function u of p may be expanded as

$$u(p)=\sum_{n=0}^{\infty}\hat{u}_n\Psi_n(p), \quad (2.13)$$

with pointwise convergence if $u \in C^{(0)}[p_T, p_B]$ and uniform convergence if $u \in D$. In view of property (ii) the coefficients in this expansion are given by $\hat{u}_n = \langle u, \Psi_n\rangle$. Since this formula is identical to the transform (2.9), (2.13) is the desired inverse transform.

Applying the transform (2.9) to the governing equations (2.1a) and (2.3) and using the property (2.10) results in

$$\frac{\partial\hat{\mathbf{v}}_n}{\partial t}+f\mathbf{k}\times\hat{\mathbf{v}}_n+\nabla\hat{\phi}_n=\hat{\mathbf{F}}_n, \quad (2.14a)$$

$$\frac{\partial\hat{\phi}_n}{\partial t}+\frac{1}{\lambda_n}\nabla\cdot\hat{\mathbf{v}}_n=\frac{\partial\hat{\Phi}_n}{\partial t}, \quad (2.14b)$$

which is formally equivalent to the divergent barotropic system (i.e., the shallow water equations). The eigenvalue λ_n is often written as $(gh_n)^{-1}$, with g the acceleration due to gravity and h_n the so-called "equivalent depth." As we will show, each λ_n is positive so we can define real "phase speeds" c_n by $c_n = (gh_n)^{1/2} = \lambda_n^{-1/2}$; each c_n is the (horizontal) phase speed of the single vertical mode n which has vertical structure $\Psi_n(p)$ in the stratified model. Since the solution of the stratified problem has been reduced to the superposition of solutions of barotropic problems corresponding to the various vertical modes, we refer to (2.9), (2.13) as the vertical normal mode transform pair.

c. *Properties of the transform*

The energetics of the stratified model (2.1) and the transformed model (2.14) are related by the Parseval relation

$$\langle u, v\rangle=\sum_{n=0}^{\infty}\hat{u}_n\hat{v}_n, \quad (2.15)$$

which may be obtained formally by expanding $u(p)$ and $v(p)$ and using the orthonormality of the functions Ψ_n. Taking the dot product of $\mathbf{v}$ with (2.1a) and integrating with respect to p yields the kinetic energy equation

$$\frac{\partial}{\partial t}\left(\frac{1}{2}\langle\mathbf{v},\mathbf{v}\rangle\right)+\langle\mathbf{v},\nabla\phi\rangle=\langle\mathbf{v},\mathbf{F}\rangle, \quad (2.16)$$

where for any two vectors $\mathbf{a}$ and $\mathbf{b}$ we interpret $\langle\mathbf{a}, \mathbf{b}\rangle$ as $\langle\mathbf{a}\cdot\mathbf{b}, 1\rangle$. Then using (2.15) we can write (2.16) as

$$\sum_{n=0}^{\infty}\left[\frac{\partial}{\partial t}\left(\frac{1}{2}\hat{\mathbf{v}}_n\cdot\hat{\mathbf{v}}_n\right)+\hat{\mathbf{v}}_n\cdot\nabla\hat{\phi}_n\right]=\sum_{n=0}^{\infty}\hat{\mathbf{v}}_n\cdot\hat{\mathbf{F}}_n. \quad (2.17)$$

Since (2.17) holds for each n individually, as shown by taking the dot product of (2.14a) with $\hat{\mathbf{v}}_n$, we can identify $\frac{1}{2}\hat{\mathbf{v}}_n\cdot\hat{\mathbf{v}}_n$, $\hat{\mathbf{v}}_n\cdot\nabla\hat{\phi}_n$, and $\hat{\mathbf{v}}_n\cdot\hat{\mathbf{F}}_n$ as the contributions from vertical mode n to the kinetic energy, conversion of kinetic to available potential energy, and generation of kinetic energy, respectively.

Similarly, multiplying (2.3) by ϕ, integrating and applying (2.15) yields the available potential energy equation

$$\sum_{n=0}^{\infty}\left[\frac{\partial}{\partial t}\left(\frac{1}{2}\frac{\hat{\phi}_n^2}{c_n^2}\right)+\hat{\phi}_n\nabla\cdot\hat{\mathbf{v}}_n\right]=\sum_{n=0}^{\infty}\frac{\hat{\phi}_n}{c_n^2}\frac{\partial\hat{\Phi}_n}{\partial t}. \quad (2.18)$$

Here the available potential energy is

$$\sum_{n=0}^{\infty}\frac{1}{2}\frac{\hat{\phi}_n^2}{c_n^2}=\frac{1}{2}\langle L\phi,\phi\rangle$$
$$=\frac{1}{2(p_B-p_T)}\left[\int_{p_T}^{p_B}\frac{1}{\sigma}\left(\frac{\partial\phi}{\partial p}\right)^2dp+\left(\frac{p}{R\bar{T}}\phi^2\right)_{p=p_B}\right], \quad (2.19)$$

with the last equality valid only if $Q = 0$ at the top and bottom boundaries. Since (2.18) holds for each n individually, as shown by multiplying (2.14b) by $\hat{\phi}_n$, we can identify $\frac{1}{2}\hat{\phi}_n^2/c_n^2$, $\hat{\phi}_n\nabla\cdot\hat{\mathbf{v}}_n$, and

$$\frac{\hat{\phi}_n}{c_n^2}\frac{\partial\hat{\Phi}_n}{\partial t}$$

as the contributions from vertical mode n to the available potential energy, conversion from available potential to kinetic energy, and generation of available potential energy, respectively.

The vertical structure problem (2.12) has an interesting variational formulation which is closely related to (2.19). To obtain it we define for any u and v in $C^{(1)}[p_T, p_B]$ the quantity

$$\langle u,v\rangle_E=\frac{1}{p_B-p_T}\left[\int_{p_T}^{p_B}\frac{u'(p)v'(p)}{\sigma(p)}dp+\left(\frac{p}{R\bar{T}}uv\right)_{p=p_B}\right], \quad (2.20)$$

where primes denote differentiation with respect to p. Since this quantity is symmetric, linear in each argument and satisfies $\langle u, u\rangle_E > 0$ unless $u = 0$, (2.20) defines an inner product on $C^{(1)}[p_T, p_B]$. We refer to $\langle\ ,\ \rangle_E$ as the *energy inner product* since $\frac{1}{2}\langle\phi,\phi\rangle_E$ is the available potential energy; it is related to the vertical inner product $\langle\ ,\ \rangle$ by $\langle u, v\rangle_E = \langle Lu, v\rangle$ when u and v are in D. The fact that $\langle u, v\rangle_E = \langle Lu, v\rangle$ when u and v are in D shows that L is positive definite. In particular, $0 < \langle\Psi_n, \Psi_n\rangle_E = \lambda_n$ for all n, establishing the claim made in the previous section.

The variational problem associated with the vertical structure problem consists of minimizing the functional $J[\Psi] = \langle\Psi, \Psi\rangle_E$ over all Ψ in $C^{(1)}[p_T, p_B]$ subject to the constraint $K[\Psi] = \langle\Psi, \Psi\rangle = 1$. This is equivalent to minimizing the functional $I[\Psi] = J[\Psi] - \lambda K[\Psi]$, where λ is a Lagrange multiplier for the constraint. This functional may be written as

$$I[\Psi]=\frac{1}{p_B-p_T}\int_{p_T}^{p_B}G(p,\Psi,\Psi')dp, \quad (2.21)$$

where

$$G(p,\Psi,\Psi')=\frac{(\Psi')^2}{\sigma}+\left(\frac{\alpha p\Psi^2}{R\bar{T}}\right)'-\lambda\Psi^2, \quad (2.22)$$

with $\alpha = (p - p_T)/(p_B - p_T)$. Setting the variation of (2.21) equal to zero (with no boundary conditions applied) leads to the Euler-Lagrange equations

$$\left.\begin{aligned}\frac{\partial G}{\partial\Psi}-\left(\frac{\partial G}{\partial\Psi'}\right)'=0, \quad p_T<p<p_B\\ \frac{\partial G}{\partial\Psi'}=0 \quad \text{at} \quad p=p_T, \quad p=p_B\end{aligned}\right\}. \quad (2.23)$$

Substituting (2.22) into (2.23) then yields the vertical structure problem (2.12). The eigenmodes $\Psi_n(p)$ thus give at least stationary values of $J[\Psi]$ subject to the constraint; a precise formulation of the variational problem is

$$\lambda_n = J[\Psi_n] = \min\{J[\Psi]:\Psi\in C^{(1)}[p_T,p_B], \langle\Psi,\Psi\rangle=1, \langle\Psi,\Psi_m\rangle=0 \ (m=0,\ldots,n-1)\}. \quad (2.24)$$

Equivalently, λ_n and Ψ_n are the minimum values and minimizing functions of the Rayleigh quotient $J[\Psi]/K[\Psi] = \langle\Psi, \Psi\rangle_E/\langle\Psi, \Psi\rangle$. Physically this says that the vertical normal modes Ψ_n correspond to states of the atmosphere for which the ratio of available potential energy to kinetic energy is minimized.

3. Implementation

For a few special stability profiles (e.g., σ = constant or $p^2\sigma$ = constant) the vertical structure problem (2.12) may be solved analytically in closed form. In most other cases [e.g., $\sigma(p)$ obtained from observations], approximate solutions must be sought. The Rayleigh-Ritz method is appropriate for this problem; its theory and error properties have been discussed in detail by Ciarlet *et al.* (1968) and Pierce and Varga (1972), among others. In this section we consider the use of the Rayleigh-Ritz method for the practical implementation of the vertical transform.

a. Solution of the vertical structure problem

The Rayleigh-Ritz method for (2.12) proceeds from the variational formulation (2.24). Recognizing that in practice we cannot minimize $J[\Psi]$ over all Ψ in $C^{(1)}[p_T, p_B]$, we choose a finite-dimensional subspace S_N of $C^{(1)}[p_T, p_B]$ and minimize $J[\Psi]$ over it instead. (The elements of S_N need not satisfy the upper and lower boundary conditions, but better results generally are obtained if they do.) Thus the Rayleigh-Ritz method defines approximate eigenvalues $\tilde{\lambda}_n$ and eigenfunctions $\tilde{\Psi}_n(p)$ by

$$\tilde{\lambda}_n = J[\tilde{\Psi}_n] = \min\{J[\Psi]:\Psi\in S_N, \langle\Psi,\Psi\rangle=1, \langle\Psi,\tilde{\Psi}_m\rangle=0 \ (m=0,\ldots,n-1)\}. \quad (3.1)$$

This variational problem leads to

$$\langle \tilde{\Psi}_n, \Psi \rangle_E = \tilde{\lambda}_n \langle \tilde{\Psi}_n, \Psi \rangle \quad \text{(all } \Psi \text{ in } S_N\text{)}, \quad (3.2)$$

which is identical to the Galerkin equation for (2.12) if the elements of S_N satisfy the boundary conditions.

To solve for $\tilde{\lambda}_n$ and $\tilde{\Psi}_n$ we fix a basis $\{\chi_0(p), \ldots, \chi_N(p)\}$ for S_N. This introduces a one-to-one correspondence between functions $u(p)$ in S_N and $(N+1)$ component vectors $\mathbf{u} = [u_0, \ldots, u_N]^T$ of their coordinates with respect to this basis. In particular, each $\tilde{\Psi}_n(p)$ corresponds to a vector $\psi_n = [\psi_{0,n}, \ldots, \psi_{N,n}]^T$ with

$$\tilde{\Psi}_n(p) = \sum_{j=0}^{N} \psi_{j,n} \chi_j(p). \quad (3.3)$$

Noting that we need only consider $\Psi = \chi_i$ $(i = 0, \ldots, N)$ in (3.2) and substituting from (3.3) we obtain

$$\sum_{j=0}^{N} \langle \chi_i, \chi_j \rangle_E \psi_{j,n} = \tilde{\lambda}_n \sum_{j=0}^{N} \langle \chi_i, \chi_j \rangle \psi_{j,n} \quad (i = 0, \ldots, N), \quad (3.4)$$

which may be written in matrix form as

$$\mathbf{A}\psi_n = \tilde{\lambda}_n \mathbf{B}\psi_n. \quad (3.5)$$

Here $\mathbf{A}$ and $\mathbf{B}$ are matrices of order $N+1$ with entries $A_{ij} = \langle \chi_i, \chi_j \rangle_E$ and $B_{ij} = \langle \chi_i, \chi_j \rangle$; this connection with the inner products guarantees that both matrices are real, symmetric and positive definite. Therefore, the generalized eigenvalue problem (3.5) has solutions $\{\tilde{\lambda}_n, \psi_n\}_{n=0}^{N}$ with the following properties.

(i) The eigenvalues $\tilde{\lambda}_n$ are real, with $0 < \tilde{\lambda}_0 < \tilde{\lambda}_1 < \cdots < \tilde{\lambda}_N$,

(ii) The eigenvectors ψ_n are orthonormal in the sense $\psi_m{}^T \mathbf{B} \psi_n = \delta_{mn}$,

(iii) The eigenvectors ψ_n form a complete set.

In view of property (i) we can define the approximate phase speeds $\tilde{c}_n = \tilde{\lambda}_n^{-1/2}$. As shown in the next section, property (ii) implies that $\langle \tilde{\Psi}_m, \tilde{\Psi}_n \rangle = \delta_{mn}$, and property (iii) implies that the functions $\Psi_n(p)$ span S_N. Thus the numerical solution obtained by the Rayleigh-Ritz method preserves much of the character of the analytical solution of (2.12).

b. *Application of the vertical transform*

Having obtained the approximate vertical structure functions $\tilde{\Psi}_n(p)$ in terms of the basis functions $\chi_j(p)$, the application of the vertical transform is now straightforward, amounting to simply a change of basis. For any function $u(p)$ in S_N we have the two representations

$$u(p) = \sum_{j=0}^{N} u_j \chi_j(p) = \sum_{n=0}^{N} \hat{u}_n \tilde{\Psi}_n(p). \quad (3.6)$$

The coefficients $\mathbf{u} = [u_0, \ldots, u_N]^T$ and $\hat{\mathbf{u}} = [\hat{u}_0, \ldots, \hat{u}_N]^T$ in these representations are related by

$$\hat{\mathbf{u}} = \mathbf{T}\mathbf{u}, \quad \mathbf{u} = \mathbf{T}^{-1}\hat{\mathbf{u}}, \quad (3.7)$$

where $\mathbf{T}^{-1}$ is the matrix whose columns are the vectors ψ_n and $\mathbf{T} = (\mathbf{B}\mathbf{T}^{-1})^T$. Thus (3.7) is a numerical representation of the transform pair (2.9), (2.13). Similarly, the inner products of any functions u and v in S_N may be expressed as

$$\langle u, v \rangle = \mathbf{v}^T \mathbf{B} \mathbf{u} = \hat{\mathbf{v}}^T \hat{\mathbf{u}} = \sum_{n=0}^{N} \hat{u}_n \hat{v}_n, \quad (3.8)$$

$$\langle u, v \rangle_E = \mathbf{v}^T \mathbf{A} \mathbf{u} = \hat{\mathbf{v}}^T \mathbf{E} \hat{\mathbf{u}} = \sum_{n=0}^{N} \tilde{\lambda}_n \hat{u}_n \hat{v}_n, \quad (3.9)$$

where $\mathbf{E} = (\mathbf{T}^{-1})^T \mathbf{A} \mathbf{T}^{-1} = \text{diag}[\tilde{\lambda}_0, \ldots, \tilde{\lambda}_N]$.

c. *Basis functions*

Many different types of functions may be used as basis functions for the Rayleigh-Ritz method. If the vertical transform is used within a numerical model which employs a series expansion (i.e., finite element or spectral) method in the vertical, the basis functions of the numerical model are the natural choice for use in computing the vertical transform (Daley, 1979; Béland *et al.*, 1983). In other applications the choice of basis functions may depend on considerations of accuracy, efficiency, storage required and ease of programming.

Piecewise polynomials (splines) have become popular for use in the Rayleigh-Ritz method (Wendroff, 1965; Birkhoff *et al.*, 1966; Johnson, 1969; Prenter, 1975). Typically, one chooses S_N as a space of piecewise cubic functions over a partition of the interval $[p_T, p_B]$, with a basis of B-splines (deBoor, 1978) which satisfy the boundary conditions; "jump" conditions arising from known discontinuities in $\sigma(p)$ may also be built into such a basis. The approximation of an arbitrary function $f(p)$ by an element g in S_N then involves solving a well-conditioned banded linear system; if f is sufficiently smooth, this approximation generally has accuracy $O(N^{-4})$. Since the matrices $\mathbf{A}$ and $\mathbf{B}$ are banded, the eigenvalue problem (3.5) may be solved efficiently, e.g. by the algorithm of Peters and Wilkinson (1969); the resulting approximate eigenvalues and eigenfunctions have accuracy $O(N^{-6})$ and $O(N^{-3})$, respectively (Ciarlet *et al.*, 1968). Greater accuracy may be obtained by using higher-order splines, at the cost of increased program complexity.

Still greater accuracy can be obtained by choosing S_N instead as the subspace of all polynomials of degree at most $N+2$ which satisfy the upper and lower boundary conditions. An analytic function $f(p)$ may be approximated by an element g of this subspace with exponential accuracy; i.e., the error in the approximation is asymptotically $O(e^{-N/N_0})$ with N_0 con-

stant. Similarly, if the true eigenfunctions $\Psi_n(p)$ are analytic then the resulting approximate eigenvalues and eigenfunctions also have exponential accuracy (Ciarlet *et al.*, 1968). There is a trade-off here between accuracy and efficiency, since the matrices involved are full. However, the high accuracy implies that N may be chosen relatively small, so the computer time and storage required are in general inconsequential. In view of the high accuracy and the ease of programming with polynomials, we use this polynomial subspace for all results reported here.

To ensure that the matrices **A** and **B** are well conditioned we construct a basis for the polynomial subspace S_N from the Chebyshev polynomials as follows. Mapping the interval $p_T \leq p \leq p_B$ onto $-1 \leq s \leq 1$ by $s = 2(p_B - p)/(p_B - p_T) - 1$, we define

$$\chi_j(p) = T_{j+2}(s) - a_j T_0(s) - b_j T_1(s), \quad (0 \leq j \leq N). \tag{3.10}$$

Here T_j is the Chebyshev polynomial of degree j, defined for $s = \cos\theta$ by $T_j(\cos\theta) = \cos(j\theta)$ so that $T_0(s) = 1$, $T_1(s) = s$ and $T_{j+2}(s) = 2sT_{j+1}(s) - T_j(s)$; further properties are given in Fox and Parker (1968). The constants a_j and b_j are chosen so that each χ_j satisfies the boundary conditions $B_T[\chi_j] = B_B[\chi_j] = 0$, resulting in

$$\left.\begin{aligned} a_j &= (-1)^j + b_j\left\{1 + \frac{2}{p_B - p_T}[1 + (-1)^j]\left(\frac{R\bar{T}}{p\sigma}\right)_{p=p_B}\right\}, \\ b_j &= (j+2)^2 \end{aligned}\right\} \tag{3.11}$$

With this basis the method is a Chebyshev-Galerkin method (Gottlieb and Orszag, 1977). To compute the elements of the matrices **A** and **B** we use a least-squares Chebyshev polynomial fit to $[p^2\sigma(p)]^{-1}$ and compute the resulting integrals exactly by Gauss-Legendre quadrature. The eigenvalue problem (3.5) is then solved by the EISPACK routine RSG, which converts it to a standard symmetric eigenvalue problem via the Cholesky decomposition of **B** and solves that problem by the QR algorithm.

Any continuous function $f(p)$ can be approximated

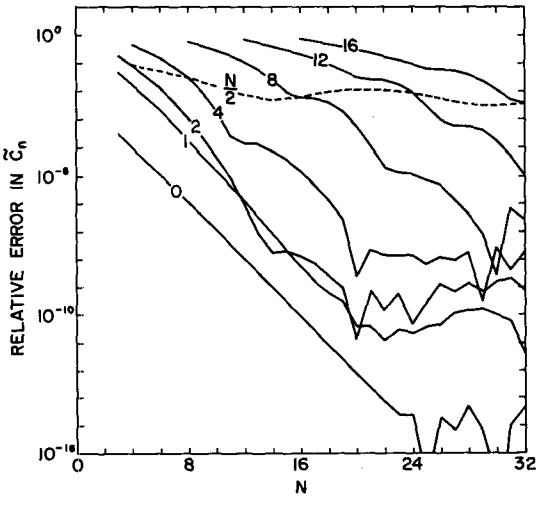

FIG. 1. Relative error $|\tilde{c}_n - c_n|/c_n$ in the phase speeds as a function of the truncation N for various vertical modes n as labeled.

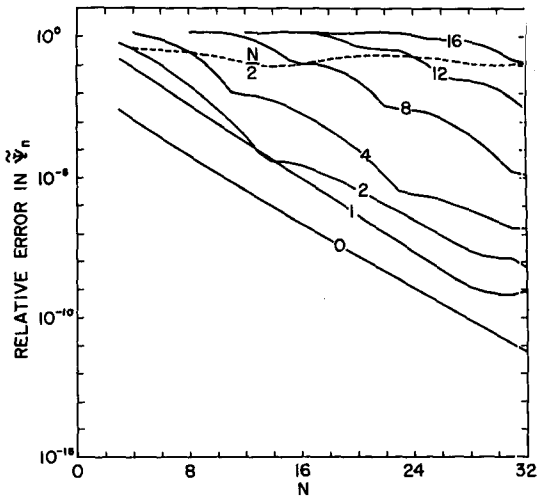

FIG. 2. Vertical norm of the error in the vertical structure functions, $\|\tilde{\Psi}_n - \Psi_n\|$, as a function of the truncation N for various vertical modes n as labeled.

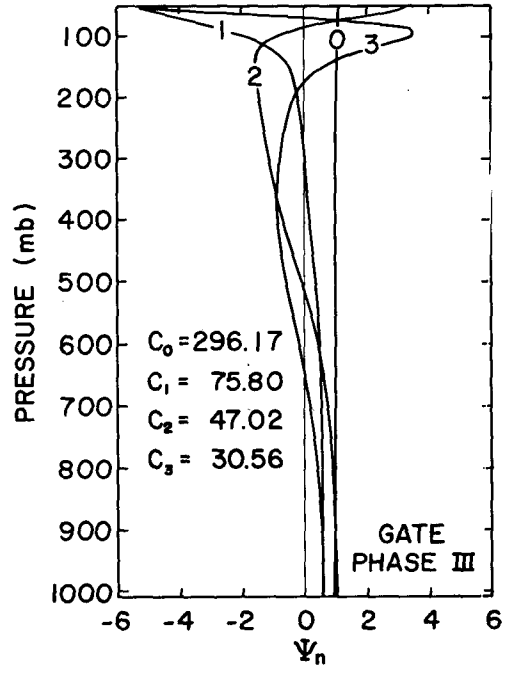

FIG. 3. First four vertical structure functions for the GATE temperature sounding of Table 4. Corresponding phase speeds (m s^{-1}) are listed at the lower left.

TABLE 1. Percent energy in mode n for reconstruction of Ψ_m from values at 12 standard levels with $p_T = 50$ mb.

		m										
n	c_n (m s^{-1})	0	1	2	3	4	5	6	7	8	9	10
0	296.17	100	0	0	0	1	4	6	4	3	0	0
1	75.80	0	105	0	8	19	59	64	51	27	23	31
2	47.02	0	0	105	2	4	11	8	5	9	19	23
3	30.56	0	0	0	100	0	0	0	1	15	34	29
4	22.92	0	0	0	4	54	15	5	0	2	1	0
5	18.88	0	0	0	8	16	19	10	1	0	4	15
6	15.58	0	0	0	1	2	8	44	8	7	1	0
7	13.55	0	0	0	1	0	0	7	29	10	0	4
8	11.66	0	0	0	1	1	1	1	9	42	2	0
9	10.31	0	0	0	0	0	0	0	0	8	30	11
10	9.21	0	0	0	1	1	0	1	1	1	19	16

by an element g of S_N by a least-squares fit in some appropriate norm. If the norm comes from an inner product then the resulting approximation,

$$g(p) = \sum_{j=0}^{N} g_j \chi_j(p), \tag{3.12}$$

to f can be computed from the linear system

$$\sum_{j=0}^{N} (\chi_i, \chi_j) g_j = (f, \chi_i), \quad (i = 0, \ldots, N), \tag{3.13}$$

where $(\ ,\ )$ denotes the inner product chosen. For the results presented here we use the Chebyshev inner product

$$(u, v) = \int_{-1}^{1} \frac{u(s)v(s)}{(1 - s^2)^{1/2}}\, ds, \tag{3.14}$$

since the resulting fit is essentially uniform, i.e., it nearly minimizes the maximum pointwise error $|f(p) - g(p)|$ (Rivlin, 1969). The linear system (3.13) is solved using the Cholesky decomposition, using Gauss-Chebyshev quadrature to evaluate the inner product (3.14). The calculations described in this section have been implemented in a set of FORTRAN 77 routines which are available from the authors.

4. Results

In this section we present solutions of the vertical structure problem obtained by the method of Section 3 and apply the vertical transform to observed tropical forcing profiles.

a. Solutions and accuracy

The accuracy of the Rayleigh-Ritz method may be illustrated by comparing the numerical solutions $\tilde{c}_n$, $\tilde{\Psi}_n$ to the true solutions c_n, Ψ_n for a case which can be solved analytically. Here we consider the case $p^2\sigma = R\Gamma$ = constant, for which (2.12) may be solved easily in log pressure coordinates (e.g., Fulton and Schubert, 1980). Figure 1 shows the relative error $|\tilde{c}_n - c_n|/c_n$ in the phase speeds as a function of the truncation N for various vertical modes n; Fig. 2 shows the corresponding error $\tilde{\Psi}_n - \Psi_n$ in the vertical structure functions measured in the vertical norm $\|\cdot\| = \langle \cdot, \cdot \rangle^{1/2}$. The values $p_B = 1010$ mb, $p_T = 100$ mb, $\Gamma = 23.79$ K and $\bar{T}(p_B) = 29.38$°C have been assumed. The exponential convergence of the method is clearly evident; for example, increasing N by 2 gives an order of magnitude improvement in $\tilde{c}_0$, and increasing N by 3 gives an order of magnitude

TABLE 2. As in Table 1 but for 11 standard levels with $p_T = 100$ mb.

		m										
n	c_n (m s^{-1})	0	1	2	3	4	5	6	7	8	9	10
0	286.87	100	0	0	0	0	0	1	6	0	6	19
1	51.61	0	100	0	0	0	2	3	4	17	10	6
2	28.85	0	0	106	0	1	5	8	15	35	27	16
3	20.58	0	0	0	107	1	1	3	14	0	13	29
4	15.23	0	0	0	0	100	1	0	0	10	0	6
5	12.34	0	0	0	0	0	91	0	0	1	1	3
6	10.22	0	0	0	0	0	2	65	1	20	0	1
7	8.74	0	0	0	0	1	2	7	18	1	13	28
8	7.64	0	0	0	0	0	4	5	2	12	2	1
9	6.80	0	0	0	0	0	1	2	4	3	36	0
10	6.12	0	0	0	0	0	0	0	3	0	1	13

improvement in $\tilde{\Psi}_0$. Machine accuracy for $\tilde{c}_0$ is reached near $N = 24$ and roundoff error affects the solutions somewhat for larger N. The dashed curves indicate that for modes $n = 0, \ldots, N/2$ the eigenvalues and eigenfunctions have relative errors at most about 0.5–1.0 and 10–20%, respectively. From this point on, only numerical solutions will be considered ($N = 32$ unless otherwise specified) and hence the tildes on $\tilde{c}_n$ and $\tilde{\Psi}_n$ will be dropped.

A constant Γ atmosphere is only a first approximation to reality. In the tropics Γ typically varies from about 40 K in the lower troposphere (~800 mb), with lower values near the surface, to about 10 K in the upper troposphere (~250 mb), with much higher values in the stratosphere. Figure 3 shows the first four vertical structure functions for the GATE temperature sounding of Table 4; phase speeds for the higher modes appear in Table 5. Comparison with solutions for much larger N indicates that the convergence of c_n and Ψ_n for this basic state is exponential but slower than for the constant Γ case considered above. The mode $n = 0$ is referred to as the external mode since it has no zeros (nodes) internal to the atmosphere; the modes $n = 1, 2, \cdots$ are referred to as internal modes, with mode n having n zeros internal to the atmosphere.

b. Sampling and aliasing

Measuring an atmospheric variable such as wind or geopotential amounts to sampling a continuous function of pressure at discrete levels, which inherently limits the amount of vertical structure which can be resolved by the data. To examine the effects of this sampling we evaluated the vertical structure functions $\Psi_m(p)$ at various discrete levels and then projected this "data" back onto the vertical modes. The results of these calculations are presented in Tables 1–3, which give the energy per mode (square of the spectral coefficient) as a percentage of the input energy 1.

For Table 1, 12 standard levels [denoted by (s) in Table 4] from the surface $p_B = 1010$ mb to the top $p_T = 50$ mb were used. These levels do not give enough resolution in the upper troposphere and stratosphere to adequately represent Ψ_m for $m \gtrsim 4$. This leads to significant aliasing; i.e., Ψ_m for larger m projects a significant amount of energy onto the lower modes, especially the first internal mode. This aliasing is reduced somewhat by placing the top at $p_T = 100$ mb as in Table 2, since this eliminates the stratosphere where the vertical structure functions are highly oscillatory. Still better results are obtained by sampling at levels equally spaced in log pressure as in Table 3. This spacing is suggested by the fact that the zeros of the vertical structure functions are equally spaced in log pressure when Γ is constant; when Γ is not constant, they are equally spaced (for the higher modes) in $x = \int_p^{p_B} (R\Gamma)^{1/2}(dp/p)$ (Courant and Hilbert, 1953, p. 337), which is nearly proportional to log pressure. These results indicate that without a careful choice of sampling levels, aliasing may give misleading information about the vertical modes present in observational data. Since the various modes differ significantly in their dynamics due to their different phase speeds (and, hence, different Rossby radii), this effect may influence any conclusions drawn from the data.

c. Application to tropical data

Vertical transforms of global data have been computed by Kasahara and Puri (1981) using the normal modes of a numerical model. Here we use the method described in Section 3 to transform observed tropical forcing profiles. The data for this application was provided by M. Yanai (personal communication, 1984) and is given in Table 4. It consists of two data sets: Marshall Islands and GATE. In addition to a mean temperature profile, each data set consists of time mean profiles of apparent heat source

TABLE 3. As in Table 1 but for 12 levels equally spaced in log(p).

		m										
n	c_n (m s^{-1})	0	1	2	3	4	5	6	7	8	9	10
0	296.17	100	0	0	0	0	0	0	0	0	0	0
1	75.80	0	100	0	0	0	0	0	0	1	1	3
2	47.02	0	0	100	0	0	0	0	0	0	1	1
3	30.56	0	0	0	100	0	0	0	0	1	3	6
4	22.92	0	0	0	0	99	0	0	1	1	5	4
5	18.88	0	0	0	0	0	99	0	1	6	9	17
6	15.58	0	0	0	0	0	0	101	2	5	16	5
7	13.55	0	0	0	0	0	0	0	109	5	1	4
8	11.66	0	0	0	0	0	0	0	0	66	1	10
9	10.31	0	0	0	0	0	0	0	2	12	19	6
10	9.21	0	0	0	0	0	0	0	2	13	14	39

TABLE 4. Physical space profiles of $\bar{T}$ (°C), Q_1 (°C day^{-1}) and Z (10^{-11} s^{-2}) as functions of p (mb) (s denotes the standard levels used in Section 4b).

	Marshall Islands mean			GATE mean			GATE disturbed		GATE undisturbed	
p	$\bar{T}$	Q_1	Z	$\bar{T}$	Q_1	Z	Q_1	Z	Q_1	Z
50(s)	−60.63	0.00	0.00	−62.22	0.00	0.00	0.00	0.00	0.00	0.00
100(s)	−73.42	1.46	8.98	−75.46	0.12	−0.45	0.08	−2.62	0.15	0.79
150(s)	−68.51	2.65	9.12	−69.07	−0.53	0.40	−0.67	3.61	−0.44	−1.44
200(s)	−55.42	2.54	6.74	−56.00	−0.77	4.10	−0.02	11.35	−1.26	−0.07
250(s)	−43.37	2.85	4.10	−43.76	0.40	3.20	1.81	8.27	−0.55	0.27
300(s)	−33.22	4.29	2.51	−33.33	1.84	−1.19	3.90	−4.02	0.46	0.43
350	−24.82	5.38	1.92	−24.85	2.79	−6.72	5.26	−14.19	1.15	−2.42
400(s)	−17.66	6.01	2.04	−17.89	2.98	−7.68	5.44	−13.87	1.34	−4.11
450	−11.73	6.39	3.14	−12.08	3.09	−3.77	5.26	−7.49	1.64	−1.62
500(s)	−6.71	6.42	4.09	−7.34	3.54	0.44	5.48	−2.86	2.24	2.34
550	−2.25	6.17	2.70	−3.28	4.04	1.96	5.92	−1.82	2.78	4.13
600	1.68	5.60	0.68	0.39	4.18	1.48	6.05	−1.60	2.93	3.25
650	5.40	4.73	0.81	3.98	3.94	0.61	5.65	−1.15	2.80	1.63
700(s)	8.78	4.07	3.56	7.55	3.68	0.72	5.20	0.04	2.66	1.11
750	11.75	3.73	5.03	10.78	3.59	2.25	4.94	3.49	2.69	1.55
800	14.41	3.33	3.44	13.54	3.61	3.33	4.75	5.26	2.84	2.22
850(s)	16.90	2.66	1.20	15.96	3.37	1.39	4.25	2.95	2.78	0.48
900	19.69	1.80	−1.81	18.42	2.55	−3.99	3.17	−2.50	2.14	−4.85
950	22.75	0.93	−5.24	21.28	1.17	−9.02	1.35	−8.89	1.05	−9.09
1000(s)	26.08	0.12	−6.94	24.60	0.08	−10.32	−0.03	−12.10	0.16	−9.29
1010(s)	26.78	0.00	−7.00	25.30	0.00	−10.36	0.00	−12.20	0.00	−9.30

$$Q = Q_1 \equiv c_p\left[\frac{\partial \bar{T}}{\partial t} + \overline{\mathbf{v}\cdot\nabla T} + \bar{\omega}\left(\frac{\partial \bar{T}}{\partial p} - \frac{R\bar{T}}{pc_p}\right)\right] \quad (4.1)$$

and apparent vorticity source

$$\mathbf{k}\cdot\nabla\times\mathbf{F} = Z \equiv \frac{\partial \bar{\zeta}}{\partial t} + \nabla\cdot[(\bar{\zeta}+\bar{f})\bar{\mathbf{v}}] + \mathbf{k}\cdot\nabla\times\left(\bar{\omega}\frac{\partial \bar{\mathbf{v}}}{\partial p}\right), \quad (4.2)$$

where $\bar{\zeta} = \mathbf{k}\cdot\nabla\times\bar{\mathbf{v}}$ and the overbar now denotes a horizontal average. The mean Marshall Islands profiles result from averaging 383 analysis times and have been used in the studies of Yanai *et al.* (1973), Yanai *et al.* (1976) and Chu *et al.* (1981). The mean GATE profiles result from averaging 145 analysis times and are a by-product of the study of Sui and Yanai (1984)[1]. In addition, the GATE data has been partitioned into disturbed (53 analysis times) and undisturbed (92 analysis times) situations based on satellite-derived upper-level cloudiness.

The profiles of Q_1 and Z for the Marshall Islands and GATE are displayed in Fig. 4. In terms of Q_1 the GATE region is less active in the mean than the Marshall Islands region. In fact, the Marshall Islands mean Q_1 closely resembles the GATE disturbed Q_1. However, in terms of Z, the GATE region seems quite active. An interesting overall difference between the Q_1 and Z profiles is the more complicated vertical structures associated with Z. This difference is important in determining which vertical modes are excited by the two apparent sources.

The spectral space representations (with $N = 32$ and $p_T = 50$ mb) of the apparent heat and vorticity sources are given in Table 5. We have also constructed similar tables (not shown) for different truncations N (e.g. $N = 8$, 16) and different model tops (e.g., $p_T = 25$, 100 mb); the differences with Table 5 are rather small as long as one views the spectral representation in terms of the phase speed c rather than the mode index n. Perhaps the most striking feature of Table 5 is the difference in the width of the spectra for Q_1 and Z, with Q_1 being projected primarily onto the narrow range $30 < c < 300$ m s^{-1} and Z onto the broad range $7 < c < 300$ m s^{-1}.

According to geostrophic adjustment theory, for a given latitude and horizontal scale, the atmospheric response to given normalized vertical modes of apparent heat source becomes smaller as the Rossby radius c_n/f increases. Conversely, the atmospheric response to given normalized vertical modes of apparent vorticity source becomes smaller as c_n/f decreases. Thus, if the spectra of Q_1 and Z were flat, the atmosphere would respond more to the high-order modes of Q_1 and the low-order modes of Z. However, since Q_1 projects so strongly on the low-order modes (see Table 5), most of the atmospheric response to heating should be in these same low-order modes. Since Z projects onto such a broad

[1] The data used by Sui and Yanai (1984) are in turn based on the upper-air objective wind analysis of K. Ooyama and J. H. Chu (see Esbensen *et al.*, 1982, for a brief description) and the objective thermodynamic analysis of Esbensen and Ooyama (1983).

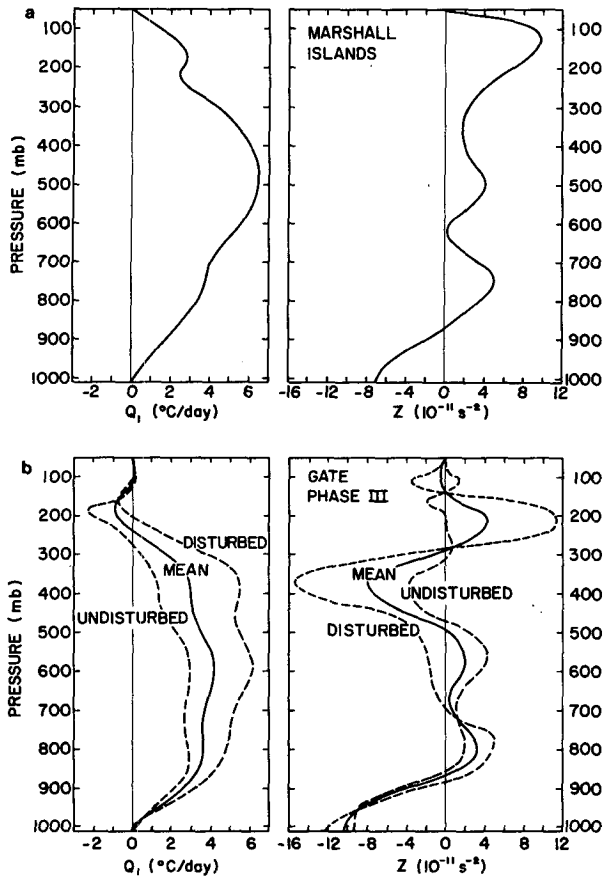

FIG. 4. Vertical profiles of the apparent heat source Q_1 and the apparent vorticity source Z for the Marshall Islands (a) and for GATE (b).

range of c_n, the atmosphere tends to respond to the low-order modes of Z. Since the horizontal scale of a typical cloud cluster is usually small compared to c_n/f for low-order modes, the atmospheric response to Z is "efficient" while the atmospheric response to Q_1 is "inefficient." However, to determine which apparent source actually yields the larger atmospheric response, one must compare the rates at which the two sources operate. This comparison is outside the scope of this study.

With the data at hand the generation of kinetic and available potential energy can not be determined, as they involve products of forcing terms with perturbation fields which are not known. Nevertheless, we can compute the quantity $(\hat{\Phi}_t/c)^2$ which is shown in Fig. 5 as a function of the phase speed c. If the time scale of the heating is short enough for it to be regarded as impulsive, then the curves in Fig. 5 give the relative distribution of initial available potential energy for the given Q_1 profiles. The sharp spectral peak then gives some justification for studies such as those of Gill (1980) and Silva Dias *et al.* (1983) which use equatorial β-plane shallow water models with $c \approx 50$ m s^{-1}. This discussion complements that of Geisler and Stevens (1982) which considered the projection of an idealized heating profile onto the normal modes of an atmosphere with constant static stability.

5. Concluding remarks

The theory of vertical normal mode transforms has been reviewed. A variational formulation which

TABLE 5. Spectral space profiles of c_n (m s^{-1}), $\partial\hat{\Phi}_n/\partial t$ (m^2 s^{-2} day^{-1}) and $\hat{Z}_n$ (10^{-11} s^{-2}) as functions of the vertical mode index n.

	Marshall Islands mean			GATE mean			GATE disturbed		GATE undisturbed	
n	c_n	$\lvert\partial\hat{\Phi}_n/\partial t\rvert$	$\lvert\hat{Z}_n\rvert$	c_n	$\lvert\partial\hat{\Phi}_n/\partial t\rvert$	$\lvert\hat{Z}_n\rvert$	$\lvert\partial\hat{\Phi}_n/\partial t\rvert$	$\lvert\hat{Z}_n\rvert$	$\lvert\partial\hat{\Phi}_n/\partial t\rvert$	$\lvert\hat{Z}_n\rvert$
0	296.66	967	2.617	296.17	614	1.002	948	1.758	391	0.566
1	77.22	562	1.046	75.80	199	0.451	376	0.722	81	0.294
2	46.66	541	2.208	47.02	311	0.478	514	0.579	175	0.419
3	31.07	55	0.553	30.56	95	0.098	116	0.747	81	0.277
4	23.36	31	0.138	22.92	43	0.117	18	2.353	59	1.171
5	18.91	11	1.096	18.88	1	0.899	9	0.108	8	1.479
6	15.72	11	1.089	15.58	9	2.293	23	3.576	1	1.555
7	13.53	9	0.606	13.55	22	2.076	37	3.354	12	1.340
8	11.67	2	0.298	11.66	13	0.484	13	0.036	13	0.784
9	10.31	1	0.517	10.31	3	0.445	10	1.318	2	0.058
10	9.20	1	0.931	9.21	7	0.059	10	0.462	5	0.172
11	8.14	1	1.205	8.14	3	1.492	5	2.802	2	0.737
12	7.22	4	0.898	7.22	6	1.486	5	1.790	6	1.310
13	6.40	2	0.567	6.41	1	0.634	1	0.312	1	0.816
14	5.72	0	0.133	5.73	2	0.606	3	0.888	1	0.443
15	5.16	1	0.024	5.16	2	0.498	2	0.769	2	0.341
16	4.68	0	0.086	4.68	0	0.309	0	0.243	0	0.346
17	4.27	1	0.175	4.27	1	0.155	2	0.326	1	0.056
18	3.92	0	0.199	3.92	0	0.111	0	0.103	0	0.113
19	3.61	0	0.172	3.62	0	0.064	0	0.135	0	0.024
20	3.34	1	0.197	3.33	0	0.055	0	0.187	0	0.021

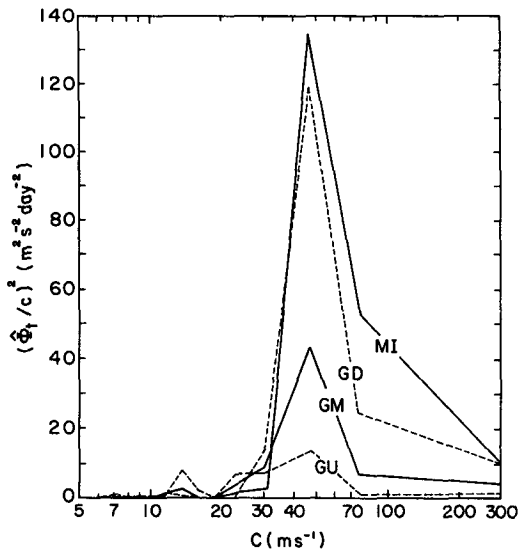

FIG. 5. Plots of $(\hat{\Phi}_t/c)^2$ as a function of c for the Marshall Islands (MI), GATE mean (GM), GATE disturbed (GD) and GATE undisturbed (GU) apparent heat sources.

is closely connected with the energetics of the atmosphere leads to the Rayleigh-Ritz method for implementing the transform in practice. With polynomial basis functions this method gives solutions with exponential order of accuracy. Transforms of observed tropical forcing profiles show that the forcing of the mass field occurs primarily for vertical modes with phase speeds in the range 30–300 m s^{-1}, while significant forcing of the wind field occurs for phase speeds as low as 7–8 m s^{-1}. Sensitivity studies indicate that spectral space profiles in terms of the phase speed c are relatively independent of the truncation N and the assumed top pressure p_T used, but that significant aliasing onto the first few modes can occur if the physical space profile is not sampled at optimum levels.

When the top of the model atmosphere is placed at $p_T = 0$ the governing equations become singular there. Depending on the basic state $\bar{T}(p)$, the spectrum of phase speeds may then become partly continuous (e.g. Eckart, 1960, Chap. 6; Jacobs and Wiin-Nielsen, 1966). The sum over discrete modes must then be replaced by an integral over the continuous spectrum, in much the same way that the Fourier series of a function approaches its Fourier transform in the limit as the period of the function approaches infinity. For the atmosphere, the distinguishing characteristic between a discrete and continuous spectrum appears to be whether the basic state temperature vanishes or approaches a finite limit at the top of the atmosphere. We are presently investigating the theory and implementation of such continuous vertical normal-mode transforms.

Acknowledgments. We wish to thank P. Silva Dias, M. DeMaria and D. Stevens for their helpful comments and M. Yanai for kindly providing both the Marshall Islands and GATE data. We are also indebted to Odilia Panella for her help in preparing the manuscript.

This work was supported by the National Science Foundation under Grant ATM-8207563 and the Naval Air Systems Command under ONR Contract N00014-84-C-0591. Acknowledgment is also made to the National Center for Atmospheric Research, which is sponsored by the National Science Foundation, for computer time used in this research.

REFERENCES

Béland, M., J. Côté and A. Staniforth, 1983: The accuracy of a finite-element vertical discretization scheme for primitive equation models: Comparison with a finite difference scheme. *Mon. Wea. Rev.*, **111**, 2298–2318.

Birkhoff, G., C. deBoor, B. Swartz and B. Wendroff, 1966: Rayleigh-Ritz approximation by piecewise cubic polynomials. *SIAM J. Numer. Anal.*, **3**, 188–203.

Chapman, S., and R. S. Lindzen, 1970: *Atmospheric Tides.* Gordon-Breach, 200 pp.

Chu, J.-H., M. Yanai and C.-H. Sui, 1981: Effects of cumulus convection on the vorticity field in the tropics. Part I: The large-scale budget. *J. Meteor. Soc. Japan*, **59**, 535–546.

Ciarlet, P. G., M. H. Schultz and R. S. Varga, 1968: Numerical methods of high-order accuracy for nonlinear boundary value problems, III. Eigenvalue problems. *Numer. Math.*, **12**, 120–133.

Courant, R., and D. Hilbert, 1953: *Methods of Mathematical Physics, Vol. 1.* Wiley-Interscience, 561 pp.

Daley, R., 1979: The application of nonlinear normal mode initialization to an operational forecast model. *Atmos.-Ocean*, **17**, 97–124.

——, 1981: Normal mode initialization. *Rev. Geophys. Space Phys.*, **19**, 450–468.

deBoor, C., 1978: *A Practical Guide to Splines.* Springer-Verlag, 392 pp.

Eckart, C., 1960: *Hydrodynamics of Oceans and Atmospheres.* Pergamon, 290 pp.

Esbensen, S. K., and K. V. Ooyama, 1983: An objective analysis of temperature and relative humidity data over the B and A/B ship arrays during Phase III of GATE. 87 pp. [Available from S. K. Esbensen, Department of Atmospheric Sciences, Oregon State University, Corvallis, OR, 97331.]

——, E. I. Tollerud and J.-H. Chu, 1982: Cloud-cluster-scale circulations and the vorticity budget of synoptic-scale waves over the eastern Atlantic intertropical convergence zone. *Mon. Wea. Rev.*, **110**, 1677–1692.

Fox, L., and I. B. Parker, 1968: *Chebyshev Polynomials in Numerical Analysis.* Oxford, 205 pp.

Fulton, S. R., and W. H. Schubert, 1980: Geostrophic adjustment in a stratified atmosphere. Atmos. Sci. Paper No. 326, Department of Atmospheric Science, Colorado State University, Fort Collins, CO, 80523, 97 pp.

Geisler, J. E., and D. E. Stevens, 1982: On the vertical structure of damped steady circulation in the tropics. *Quart. J. Roy. Meteor. Soc.*, **108**, 87–93.

Gill, A. E., 1980: Some simple solutions for heat-induced tropical circulation. *Quart. J. Roy. Meteor. Soc.*, **106**, 447–462.

Gottlieb, D., and S. A. Orszag, 1977: *Numerical Analysis of Spectral Methods.* NSF-CBMS Monogr. No. 26, Soc. Ind. and Appl. Math., 172 pp. [NTIS No. AD-A056 922.]

Hack, J. J., and W. H. Schubert, 1981: Lateral boundary conditions for tropical cyclone models. *Mon. Wea. Rev.*, **109,** 1404–1420.

Jacobs, S. J., and A. Wiin-Nielsen, 1966: On the stability of a barotropic basic flow in a stratified atmosphere. *J. Atmos. Sci.*, **23,** 682–687.

Johnson, O. G., 1969: Error bounds for Sturm-Liouville eigenvalue approximations by several piecewise cubic Rayleigh-Ritz methods. *SIAM J. Numer. Anal.*, **6,** 317–333.

Kasahara, A., and K. Puri, 1981: Spectral representation of three-dimensional global data by expansion in normal mode functions. *Mon. Wea. Rev.*, **109,** 37–51.

——, and Y. Shigehisa, 1983: Orthogonal vertical normal modes of a vertically staggered discretized atmospheric model. *Mon. Wea. Rev.*, **111,** 1724–1735.

Lamb, H., 1932: *Hydrodynamics.* sixth ed, Dover, 732 pp.

Lindzen, R. S., 1967: Planetary waves on beta-planes. *Mon. Wea. Rev.*, **95,** 441–451.

Oliger, J., and A. Sundström, 1978: Theoretical and practical aspects of some initial boundary value problems in fluid dynamics. *SIAM J. Appl. Math.*, **35,** 419–446.

Peters, G., and J. H. Wilkinson, 1969: Eigenvalues of $Ax = \lambda Bx$ with band symmetric A and B. *Comp. J.*, **12,** 398–404.

Pierce, J. G., and R. S. Varga, 1972: Higher order convergence results for the Rayleigh-Ritz method applied to eigenvalue problems, I. Estimates relating Rayleigh-Ritz and Galerkin approximations to eigenfunctions. *SIAM J. Numer. Anal.*, **9,** 137–151.

Prenter, P. M., 1975: *Splines and Variational Methods.* Wiley, 323 pp.

Rivlin, T. J., 1969: *An Introduction to the Approximation of Functions.* Dover, 150 pp.

Siebert, M., 1961: Atmospheric tides. *Advances in Geophysics,* Vol. 7, Academic Press, 105–187.

Silva Dias, P. L., W. H. Schubert and M. DeMaria, 1983: Large-scale response of the tropical atmosphere to transient convection. *J. Atmos. Sci.*, **40,** 2689–2707.

Sneddon, I. H., 1972: *The Use of Integral Transforms.* McGraw-Hill, 539 pp.

Stakgold, I., 1979: *Green's Functions and Boundary Value Problems.* Wiley-Interscience, 638 pp.

Sui, C.-H., and M. Yanai, 1984: Vorticity budget of the GATE A/B area and its interpretation. *Proc. 15th Conf. on Hurricanes and Tropical Meteorology,* Miami, Amer. Meteor. Soc., 465–472.

Taylor, G. I., 1936: The oscillations of the atmosphere. *Proc. Roy. Soc. London,* **A156,** 318–326.

Temperton, C., 1984: Orthogonal vertical normal modes for a multilevel model. *Mon. Wea. Rev.*, **112,** 503–509.

Wendroff, B., 1965: Bounds for eigenvalues of some differential operators by the Rayleigh-Ritz method. *Math. Comp.*, **19,** 218–224.

Wiin-Nielsen, A., 1971a: On the motion of various vertical modes of transient, very long waves, part I. Beta plane approximation. *Tellus,* **23,** 87–98.

——, 1971b: On the motion of various vertical modes of transient, very long waves, part II. The spherical case. *Tellus,* **23,** 207–217.

Yanai, M., S. K. Esbensen and J.-H. Chu, 1973: Determination of bulk properties of tropical cloud clusters from large-scale heat and moisture budgets. *J. Atmos. Sci.*, **30,** 611–627.

——, J.-H. Chu, T. E. Stark and Ts. Nitta, 1976: Response of deep and shallow tropical maritime cumuli to large-scale processes. *J. Atmos. Sci.*, **33,** 976–991.